



Fiber-optic ultrasonic hydrophone using short Fabry–Perot cavity with multilayer reflectors deposited on small stub



Kyung-Su Kim^{*}, Yosuke Mizuno, Kentaro Nakamura

Precision and Intelligence Laboratory, Tokyo Institute of Technology, 4259 Nagatsuta-cho, Midori-ku, Yokohama 226-8503, Japan

ARTICLE INFO

Article history:

Received 3 April 2013

Received in revised form 12 December 2013

Accepted 16 December 2013

Available online 21 December 2013

Keywords:

Ultrasonic hydrophone

Optical fiber sensor

Band-pass filter

Dielectric multilayer film

Fabry–Perot resonator

ABSTRACT

A fiber-optic probe with dielectric multilayer films deposited on a small stub is studied for mega-hertz ultrasonic-wave detection in water. The small stub with a short Fabry–Perot cavity and distributed reflectors is attached on the fiber end. The structure is mechanically strong and withstands intense ultrasonic pressure. Ultrasonic waves at 1.56 MHz are successfully detected in water with a good signal-to-noise ratio. The working principle and the characteristics are studied by comparing the ultrasonic sensitivity with that of a conventional piezoelectric hydrophone. The distance response and directional response are also investigated.

© 2013 Elsevier B.V. All rights reserved.

1. Introduction

Mega-hertz ultrasonic-wave detection in liquids is of great significance because of its broad application capabilities in both biomedical and industrial fields. Piezoelectric hydrophones based on polyvinylidene difluoride (PVDF) needles [1–5] have been commonly used, but they are fragile and sometimes broken by high sound pressure. Besides, the length of their output cables is limited by the high electric impedance. As alternative sensors, fiber-optic ultrasonic sensors have been developed with such advantages as high spatial resolution, durability against high sound pressure, and immunity to electromagnetic interference [6–23]. Their typical examples include ultrasonic sensors based on (1) reflection at the fiber end [6–12], (2) fiber Bragg gratings (FBGs) [13–16], (3) fiber Fabry–Perot (FFP) resonators with mirrors [17–20], and (4) FFP resonators with distributed Bragg reflectors (DBRs) [21–23]. In the first example, the refractive-index modulation of surrounding liquid due to ultrasound field is detected as the change in the reflection coefficient at the fiber end surface [6–12]. This method provides the information on the absolute sound pressure since the relationship between the refractive index change and the sound pressure is already known quantitatively. This was successfully applied to the measurement of shock waves in water with its characteristics, but suffered from its low sensitivity, though some techniques including tapering have been developed to improve the sensitivity. Ultrasonic sensors using FBGs, which act as the

optical-band pass reflectors, have much higher sensitivity to ultrasonic field, but the spatial resolution in the direction of fiber axis is insufficient because the FBGs need to be long enough to have a steep slope in the band-pass spectra [13–16]. Developing ultrasonic sensors using FFP resonators with mirrors is one of the effective methods to improve the spatial resolution, but they suffer from the complicated fabrication process and the fragile structure [17–20]. In the last example, the mirrors of the FFP sensors are replaced by multilayer reflectors to ensure the robustness of the sensing head exploiting their established deposition method [21–23]. This structure has been shown to have moderate sensitivity with high spatial resolution as a fiber-optic ultrasonic sensor, however, it is hard to directly deposit multilayer reflectors at the end of an optical fiber since the sensor head is extremely fragile.

In this study, the sensor based on “band-pass filter (BPF) on a fiber end” (BOF) [24] is investigated as an ultrasonic probe. The BOF is fabricated with a conventional deposition technique on a firm small stub, which is connected to a fiber-optic cable. This structure provides high mechanical durability and enables a less expensive production. The BOF has been studied as a temperature sensor [24] and a sensor for external mechanical loading [25]. The authors’ group has found a possibility to use the BOF as a refractive index sensor [26]. We present a trial to apply the BOF sensor for mega-hertz ultrasonic-wave detection in water. We experimentally show that ultrasonic waves at 1.56 MHz are successfully detected in water with a good signal-to-noise ratio (SNR). From the results, we study the working principle and the characteristics by comparing the ultrasonic sensitivity with that of a conventional

^{*} Corresponding author. Tel.: +81 459245052.

E-mail address: kskim@sonic.pi.titech.ac.jp (K.-S. Kim).

hydrophone. We also measure its distance response and directional response.

2. Principle

2.1. Structure of BOF

The key part of our fiber-optic probe is known as the BOF, which consists of the FFP resonators with DBRs. The BOF, however, is composed of dielectric multilayer films (DMFs) deposited on a small stub made of crystallized glass, which is connected to the optical fiber end and fixed with a sleeve as shown in Fig. 1. The DMFs comprising SiO_2 and TiO_2 layers accumulated by ion-assisted evaporation form an optical cavity, which serves as an optical filter. The BOF has following three advantages: (1) DMFs deposited on the small stub are much easier to manufacture compared with those deposited directly on the fiber end, (2) it is suitable for mass production with low cost, and (3) its sensor head is robust owing to the lattice match of each layer, which enables high-frequency ultrasonic-wave detection without damage. Fig. 2 represents the detailed Fabry–Perot structure of the DMFs, which is composed of a cavity of 925-nm-thick SiO_2 layer and DBRs on both sides. Each DBR is composed of 4 pairs of 215-nm-thick SiO_2 ($n = 1.46$) and 215-nm-thick TiO_2 ($n = 2.22$) layers. The TiO_2 top layer protecting the whole structure is 450-nm thick.

2.2. Sensing principle

The typical reflection spectrum of the BOF is illustrated in Fig. 3(a and b), where the sharp dip is observed at 1534.1 nm. When broad-band light is injected into the BOF, it selectively eliminates a light component at a particular wavelength λ_c . If the stress is applied to the BOF, λ_c shifts in proportion to its magnitude [25]. We have also found that λ_c is sensitive to the refractive index of the media facing at the top layer of the BOF. The relation between the shift in λ_c and the refractive index has been clarified [26]. Since ultrasonic field induces stress to the BOF as well as refractive-index modulation of media (water) surrounding the BOF, the wavelength λ_c is modulated in proportion to the magnitude of the ultrasonic field applied to the BOF. It is important to reveal which of the two contributions is the more prominent in using the BOFs to detect ultrasonic waves.

3. Experiments

3.1. Setup

Fig. 4 shows the experimental setup for ultrasonic-wave detection using the BOF-based ultrasonic hydrophone, which was originally developed for high-speed measurement of refractive index [27]. A tunable laser diode (TLD) of 1550-nm band was used as a light source and its output power was fixed at 5 dBm. The output light was injected into the BOF via an optical circulator. The reflected light from the BOF was converted to an electrical signal using a photodiode (PD) with a bandwidth of over 5 MHz, and was monitored employing an oscilloscope (OSC) with a sampling

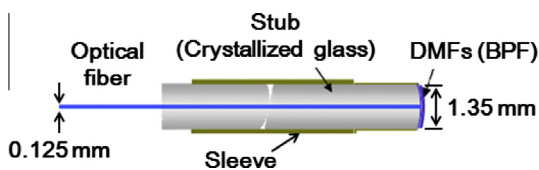


Fig. 1. Structure of the BOF-based sensor.

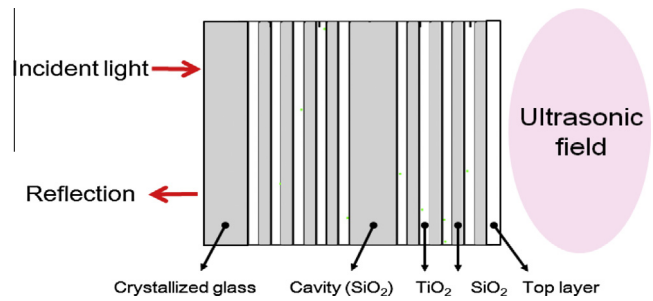


Fig. 2. Detailed layer structure of the DMFs.

rate of 250 MS/s. By applying electrical burst waves to a disk-shaped piezoelectric transducer (PZT) with a diameter of 25 mm, ultrasonic burst waves at 1.56 MHz were generated. The number of the burst was approximately 20. The end of the BOF-based ultrasonic hydrophone was fixed above the center of the PZT. Since the wavelength of the TLD was set at the center of the slope in the BOF response, the modulation in λ_c was converted into an alternative voltage at the PD.

3.2. Sensitivity

Fig. 5(a) shows the measured alternating current (AC) component of the signal voltage U_{ac} , when the optical wavelength was 1532.50 nm and the distance between the BOF end and the PZT was 50 mm. The waveform was averaged for 64 shots. For comparison, we also detected the same ultrasonic waves with a conventional needle hydrophone as shown in Fig. 5(b). The obtained waveforms were similar in shape and SNR, which indicates that the BOF-based sensor properly works as an ultrasonic hydrophone.

Fig. 6(a) represents the optical wavelength dependence of the direct current (DC) component of the signal voltage U_{dc} and that of the peak-to-peak value of U_{ac} ($\equiv U_{p-p}$). The DC component indicates the reflectivity of the BOF, while U_{p-p} shows the amplitude of the ultrasonic signal. As can be seen, if we differentiate the curve of the obtained U_{dc} with respect to optical wavelength, the shape of U_{p-p} can be obtained. The absolute value U_{p-p} became the maximum at 1533.50 and 1535.75 nm; U_{ac} at 1533.50 nm is plotted as negative values and at 1535.73 nm as positive ones, because the U_{ac} waveforms at 1533.73 nm and 1535.50 nm are out of phase with each other as shown in Fig. 6(b). The reverse of the phase is caused by the difference in the sign of the slope of the U_{dc} .

From the measurement using the piezoelectric needle hydrophone with known sensitivity, the acoustic pressure P_{in} was estimated to be 324 kPa (peak-to-peak value). To eliminate the effects of the input optical power and the sensitivity of the PD on the hydrophone characteristics, we define the sensitivity of the BOF-based hydrophone as $S_{BOF} = |U_{p-p}/U_{dc}|/P_{in}$. The sensitivity is plotted as a function of the optical wavelength as shown in Fig. 7. The maximum sensitivity of $3.43 \times 10^{-4} \text{ MPa}^{-1}$ was obtained at 1534.2 nm for the 1.56-MHz ultrasonic field.

The sensitivity to the refractive-index change of the surrounding media has already been verified in our previous study [26]. Using this value and the relationship between the sound pressure and the refractive-index change [28], we can calculate the sensitivity to ultrasonic field based on the refractive-index modulation of water facing the BOF. It was, however, calculated to be $3.95 \times 10^{-5} \text{ MPa}^{-1}$, which was almost 10 times as small as the measured sensitivity ($\approx 3.43 \times 10^{-4} \text{ MPa}^{-1}$). Consequently, we concluded that the stress applied to the BOF structure is the major principle of the ultrasonic sensitivity.

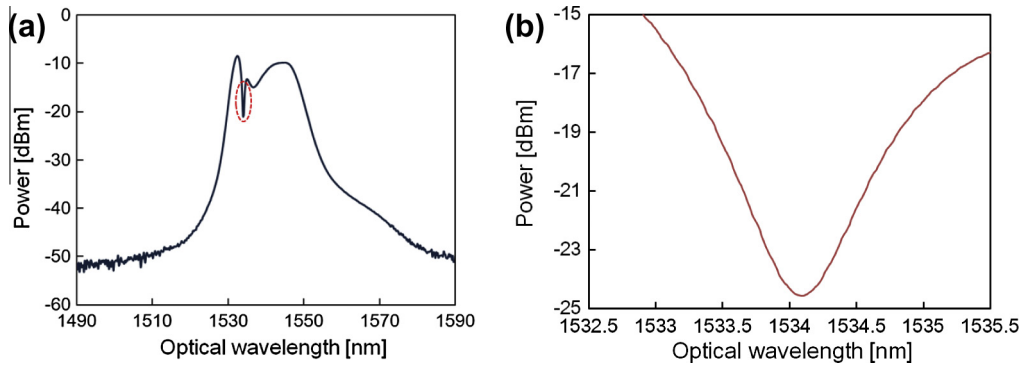


Fig. 3. (a) Typical reflection spectrum of the BOF in air, and (b) its magnified view around the dip.

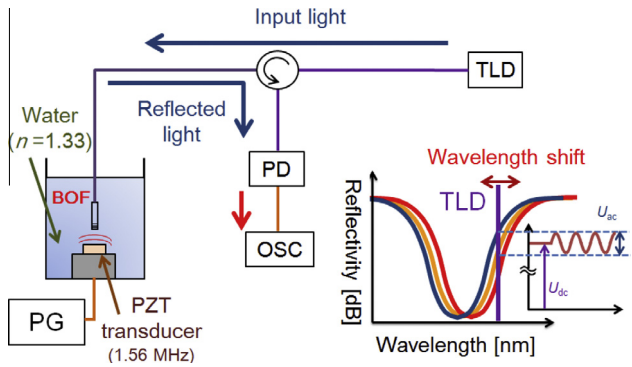


Fig. 4. Schematic experimental setup for ultrasonic-wave measurement. OSC, oscilloscope; PD, photodiode; PG, pulse generator; PZT, piezoelectric transducer; TLD, tunable laser diode.

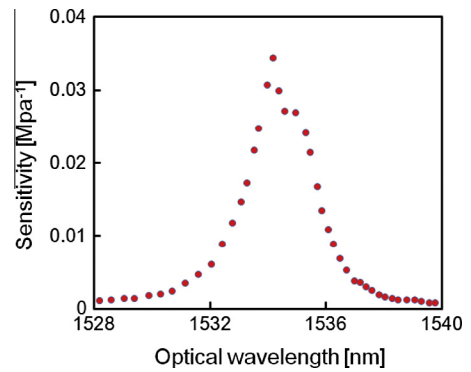


Fig. 7. Sensitivity of BOF-based ultrasonic hydrophone.

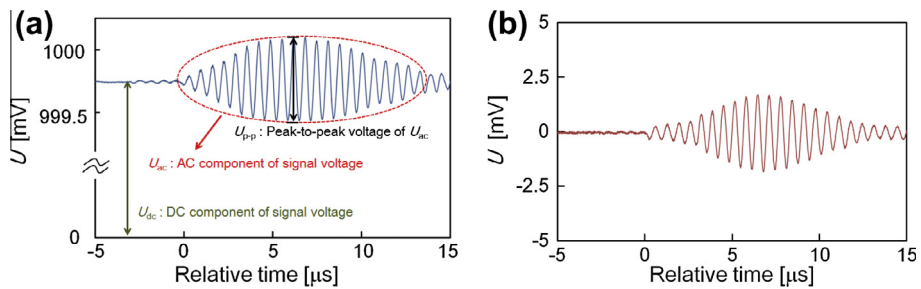


Fig. 5. U_{ac} measured with (a) the BOF-based ultrasonic hydrophone, and (b) the conventional needle hydrophone.

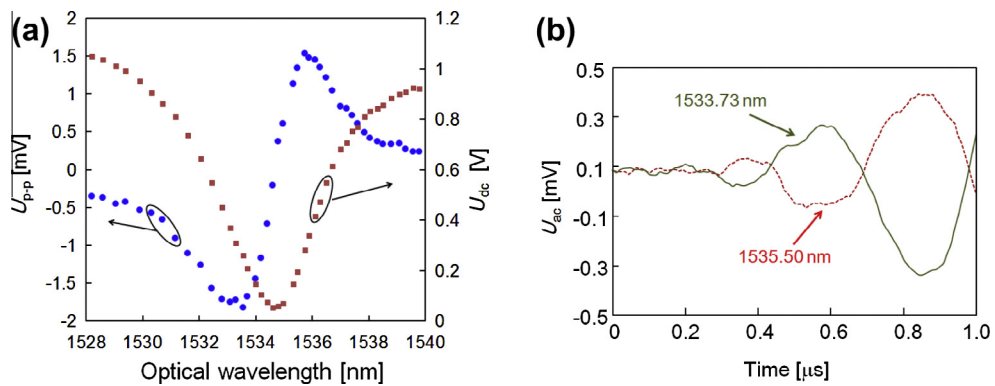


Fig. 6. (a) U_{p-p} and U_{dc} as functions of optical wavelength, and (b) waveforms of U_{ac} at 1533.50 and 1535.73 nm.

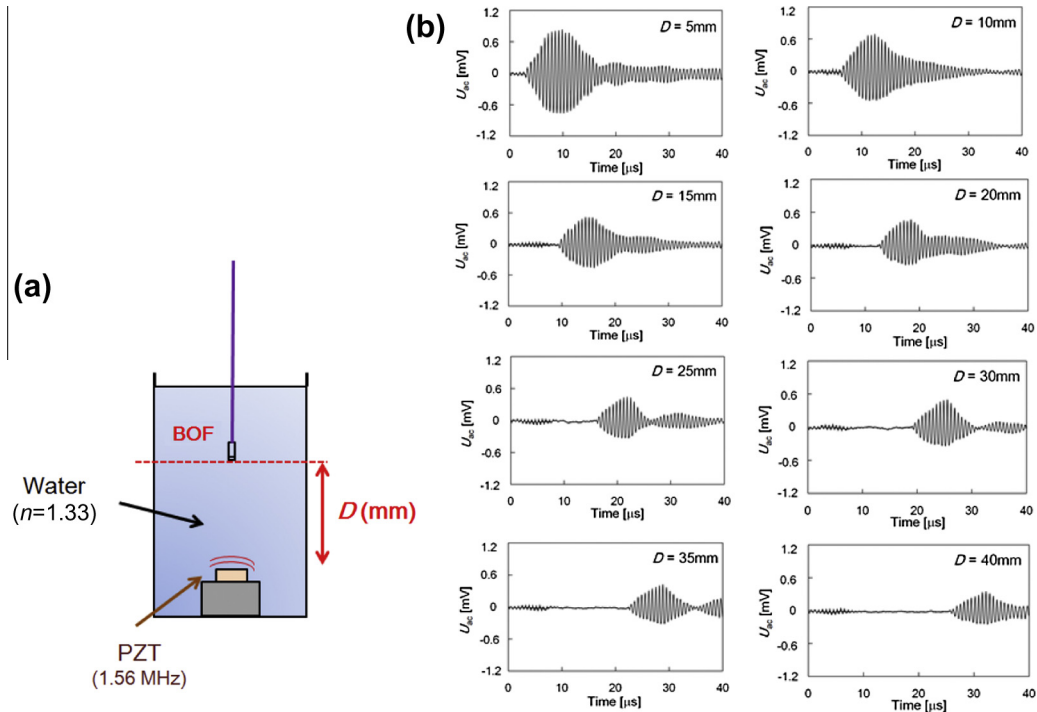


Fig. 8. (a) Schematic setup, and (b) signal waveforms under different distances.

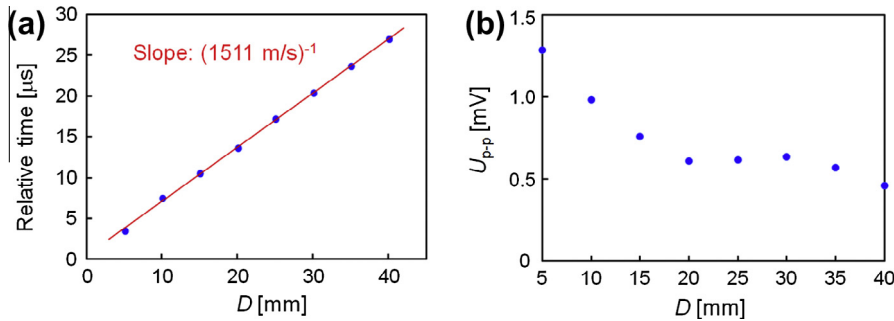


Fig. 9. (a) Relative time vs. distance; the slope indicates the reciprocal of the ultrasonic velocity in water, and (b) U_{p-p} vs. distance.

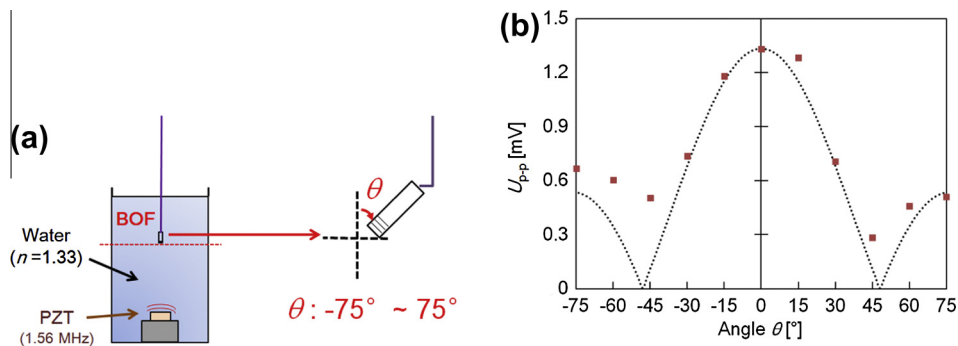


Fig. 10. (a) Schematic setup, and (b) U_{p-p} vs. angle θ ; comparison between experiment and theory.

3.3. Distance and directional response

Next, the dependence of the signal waveform on the distance D from the PZT was investigated as depicted in Fig. 8(a) to confirm that the signal is ultrasonically generated. The optical wavelength and power were fixed at 1533.50 nm and at 5 dBm, respectively.

The measurement result is shown in Fig. 8(b) as D became longer the signal waveform was delayed and its peak voltage was attenuated. Fig. 9(a) shows the relative time as a function of the distance D . Since the time was determined using the first clear peak observed in the signal waveform, the measurement error was of the order of the acoustic wavelength, approximately $\pm 0.2 \mu\text{s}$ (Refer also

to Fig. 6). The curve was almost linear and its slope was the reciprocal of 1511 m/s, which agrees well with the acoustic velocity in water at room temperature [29]. Fig. 9(b) shows the peak voltage dependence on D , where the voltage was attenuated as D became longer. The slight increase in the voltage at $D \sim 30$ mm was probably caused by the nature of the sound distribution produced by the finite radiation surface. These results also show that the BOF sensor can detect the ultrasonic signal correctly in the experiment.

Finally, we measured the dependence of the peak signal voltage on the angle θ with respect to the vertical axis to verify the directional response of the BOF as shown in Fig. 10(a). The BOF was rotated with an angular step of 15° from the vertical axis. The wavelength was 1533.50 nm, and the optical power was 5 dBm. The measured response is shown as solid squares in Fig. 10(b), which was almost symmetric with respect to the $\theta = 0^\circ$ axis. In addition to a main lobe with a width of approximately 60° , two sidelobes were observed. This is similar to the theoretical far field response of the circular sensing aperture with a diameter of 1.27 mm (dotted line), which was almost the same as the BOF sensing head with 1.35-mm diameter. Therefore, the directional response of the BOF-based ultrasonic hydrophone seems to be dominated by the diameter of the stub, though the optically sensitive part has a diameter of less than $10 \mu\text{m}$, which is the mode field diameter of the single-mode fiber. This fact implies that the ultrasonic waves were detected as the deformation of the BOF instead of the change in the refractive index of the surrounding media. The diameter of the sensing stub is required to be reduced for high frequency detection.

4. Conclusion

We demonstrated a trial to apply the BOF-based sensor to mega-hertz ultrasonic-wave detection in water. Ultrasonic waves at 1.56-MHz were experimentally detected with a good SNR. The sensitivity of the sensor at this frequency was $3.43 \times 10^{-4} \text{ MPa}^{-1}$. This value implied that the stress induced by ultrasonic waves to the BOF has significant contribution to the ultrasonic sensitivity of the BOF. We also experimentally investigated the distance response and the directional response of the BOF. The frequency responses in ultrasonic sensing using the BOF are left for future studies.

Acknowledgement

The authors are indebted to Dr. Onoda and Mr. Nakano, Watanabe Co., Ltd., Japan, for providing the BOF samples. This work was partially supported by a Grant-in-Aid for Research Activity Start-up (24860029) from the Japan Society for the Promotion of Science (JSPS), and by research grants from the Hattori–Hokokai Foundation, the Mazda Foundation, and the JFE 21st Century Foundation.

References

- [1] P.A. Lewin, Miniature piezoelectric polymer ultrasonic hydrophone probes, *Ultrasonic* 19 (1981) 213–216.

- [2] B. Granz, PVDF hydrophone for the measurement of shock waves, *IEEE Trans. Electron. Insul.* 24 (1989) 499–502.
- [3] R.C. Preston, D.R. Bacon, A.J. Livett, K. Rajendran, PVDF membrane hydrophone performance properties and their relevance to the measurement of the acoustic output of medical ultrasonic equipment, *J. Phys. E. Sci. Instrum.* 16 (1983) 786–796.
- [4] K.C. Shotton, D.R. Bacon, R.M. Quilliam, A pvdf membrane hydrophone for operation in the range 0.5–15 MHz, *Ultrasonics* 18 (1980) 123–126.
- [5] P.A. Lewin, G. Lypacewicz, R. Bautista, V. Devaraju, Sensitivity of ultrasonic hydrophone probes below 1 MHz, *Ultrasonics* 38 (2000) 135–139.
- [6] J. Staudenraus, W. Eisenmenger, Fiber-optic probe hydrophone for ultrasonic and shock-wave measurements in water, *Ultrasonics* 31 (1993) 267–273.
- [7] C. Wurster, J. Staudenraus, W. Eisenmenger, The fiber optic probe hydrophone, *Proc.-IEEE Ultrason. Symp.* 2 (1994) 941–944.
- [8] P.A. Lewin, C. Mu, C. Umchid, A. Daryoush, M. El-Sherif, Acoustic-optic, point receiver hydrophone probe for operation up to 100 MHz, *Ultrasonics* 43 (2005) 815–821.
- [9] B. Shen, Y. Wada, D. Koyama, R. Isago, Y. Mizuno, K. Nakamura, Fiber-optic ultrasonic probe based on refractive-index modulation in water, *Proc. SPIE* 7753 (2010). 77539W-1–77539W-4.
- [10] G. Wild, S. Hincley, Acousto-ultrasonic optical fiber sensor: overview and state-of-the-art, *IEEE Sens. J.* 8 (2008) 1184–1193.
- [11] S. Umchid, R. Gopinath, K. Srinivasan, P.A. Lewin, A.S. Daryoush, L. Bansal, M. El-Sherif, Development of calibration techniques for ultrasonic hydrophone probes in the frequency range from 1 to 100 MHz, *Ultrasonics* 49 (2009) 306–311.
- [12] D.C. Betz, G. Thursby, B. Culshaw, W.J. Staszewski, Acousto-ultrasonic sensing using fiber Bragg gratings, *Smart Mater. Struct.* 12 (2003) 122–128.
- [13] B. Culshaw, G. Thursby, D. Betz, B. Sorazu, The detection of ultrasound using fiber-optic sensors, *IEEE Sens. J.* 8 (2008) 1360–1367.
- [14] S. Campopiano, A. Cutolo, A. Cusano, M. Giordano, G. Parente, G. Lanza, A. Laudati, Underwater acoustic sensors based on fiber Bragg gratings, *Sensors* 9 (2009) 4446–4454.
- [15] N. Takahashi, K. Yoshimura, S. Takahashi, K. Imamura, Development of an optical fiber hydrophone with fiber Bragg grating, *Ultrasonics* 38 (2000) 581–585.
- [16] P. Morris, A. Hurrell, A. Shaw, E. Zhang, P. Beard, A Fabry–Perot fiber-optic ultrasonic hydrophone for the simultaneous measurement of temperature and acoustic pressure, *J. Acoust. Soc. Am.* 125 (2009) 3611–3622.
- [17] Y. Uno, K. Nakamura, Pressure sensitivity of a fiber-optic microprobe for high-frequency ultrasonic field, *Jpn. J. Appl. Phys.* 38 (1999) 3120–3123.
- [18] P.C. Beard, T.N. Mills, Miniature optical fibre ultrasonic hydrophone using a Fabry–Perot polymer film interferometer, *Electron. Lett.* 33 (1997) 801–803.
- [19] J.J. Alcoz, C.E. Lee, H.F. Taylor, Embedded fiber-optic Fabry–Perot ultrasound sensor, *IEEE Trans. Ultrason. Ferr.* 17 (1990) 302–306.
- [20] C. Koch, Coated fiber-optic hydrophone for ultrasonic measurement, *Ultrasonics* 34 (1996) 687–689.
- [21] V. Wilkens, C. Koch, Fiber-optic multilayer hydrophone for ultrasonic measurement, *Ultrasonics* 37 (1999) 45–49.
- [22] W. Weise, V. Wilkens, C. Koch, Frequency response of fiber-optic multilayer hydrophones: experimental investigation and finite element simulation, *IEEE Trans. Ultrason. Ferroelectrics Frequency Control* 49 (2002) 937–946.
- [23] V. Wilkens, Characterization of an optical multilayer hydrophone with constant frequency response in the range from 1 to 75 MHz, *J. Acoust. Soc. Am.* 113 (2003) 1431–1438.
- [24] S. Onoda, N. Tsukamoto, M. Ogino, K. Yamashita, O. Yumoto, K. Inoue, Y. Komatsu, A proposal of temperature sensing using a thin-film bandpass filter and dual-wavelength push–pull reflectometry, *IEEE Photonics Technol. Lett.* 20 (2008) 688–690.
- [25] S. Onoda, K. Inoue, M. Nakano, Y. Komatsu, Fiber optic multipoint pressure and temperature sensing system using BOF/DWPR, *Proc. SPIE* 8197 (2011) 819707-1–819707-6.
- [26] K.S. Kim, Y. Mizuno, M. Nakano, S. Onoda, K. Nakamura, Refractive index sensor for liquids and solids using dielectric multilayer films deposited on optical fiber end surface, *IEEE Photonics Technol. Lett.* 23 (2011) 1472–1474.
- [27] K.S. Kim, Y. Mizuno, K. Nakamura, High-speed measurement of refractive index using dielectric multilayer films deposited on optical fiber end, *Jpn. J. Appl. Phys.* 51 (2012) 080202-1–080202-2.
- [28] L. Adler, E.A. Hiedemann, Determination of the nonlinearity parameter B/A for water and m-Xylene, *J. Acoust. Soc. Am.* 34 (1962) 410–412.
- [29] G. Van Venrooij, Measurement of ultrasound velocity in human tissue, *Ultrasonics* 9 (1971) 240–242.